Int J Clin Exp Pathol 2015;8(5):4651-4661
www.ijcep.com /ISSN:1936-2625/IJCEP0005848

Original Article

Anti-fibrotic effects of the Masson pine pollen aqueous extract on hepatic fibrosis rat model

Tao Cong[1], Xue-Yuan Jin[2], Lin Zhao[3], Long Ma[4], Rui-Sheng Li[5], Ping Zhao[2], Chang-Jiang Guo[1]

[1]Department of Nutrition, Institute of Health and Environmental Medicine, Tianjin 300050, China; [2]International Center for Liver Disease Treatment, 302 Hospital of PLA, Beijing 100039, China; [3]Department of Nutrition, General Hospital of P.L.A, Beijing 100853, China; [4]The Second Artilery General Hospital of P.L.A, Beijing 100853, China; [5]The Experimental Animals Center, 302 Military Hospital of China, Beijing 100039, China

Received January 13, 2015; Accepted March 16, 2015; Epub May 1, 2015; Published May 15, 2015

Abstract: *Aim:* To observe the antifibrotic effects of Masson Pine Pollen aqueous extract. *Methods:* Adult Sprague-Dawley rats were randomly divided into control (CG), hepatic fibrosis model (MG), MPPAE low dose (LG), MPPAE high dose (HG), and MPP original powder (MPPOP; OG) groups. Each group was treated with specific protocols and sacrificed 8 weeks later. Multiple indicators such as serum transaminase, HE staining of the liver tissue, and relevant indexes to fibrosis were determined. *Results:* Severe hyperplasia of fibrous connective tissues was observed in livers of the MG group rats, while aspartate transaminase and alanine transaminase levels and collagen content obviously increased, superoxide dismutase and glutathione peroxidase activities and MMPs expression decreased, malondialdehyde (MDA) and 8-hydroxy-2'-deoxyguanosine concentrations increased, while mRNA expressions of hepatic stellate cell (HSC)-related cytokines such as transforming growth factor-β_1 and platelet-derived growth factor, transcription factors such as nuclear factor-κB p65, and signaling protein α-smooth muscle actin were all increased significantly. *Conclusions:* MPPAE effectively inhibited the fibrotic process in this CCl_4-induced hepatic fibrosis rat model. It may be associated with synergic functions of antioxidant activity, inhibitory activity on HSC proliferation, collagen synthesis, and MMPs expression induction.

Keywords: Masson pine pollen aqueous extract, hepatic fibrosis, CCl_4, antioxidant, matrix metalloproteinase

Introduction

Hepatic fibrosis is a self-healing response to chronic liver injury induced by various causes [1]. It is the common pathological basis of variant chronic liver diseases and involved in the progression of chronic liver diseases into cirrhosis. Cirrhosis is generally irreversible, but it is possible to reverse hepatic fibrosis, and timely treatment could control or even reverse the symptoms of fibrosis. Hepatic fibrosis formation is a dynamic process, and various pathogenic factors such as hepatitis viruses, schistosomiasis infection, toxic substances (e.g. alcohol, CCl_4), fat metabolic products, inflammatory factors, and reactive oxygen species (ROS) could damage liver cells and stimulate Kupffer cells to produce numerous cytokines (e.g. transforming growth factor-β_1 [TGF-β_1], platelet-derived growth factor [PDGF]) leading to the activation of hepatic stellate cells (HSCs). Then HSCs are transformed into myofibroblasts (MFBs), which are further stimulated by cytokines to upregulate collagen synthesis, increase extracellular matrix (ECM) production, inhibit protein degradation, promote protein aggregation, and finally lead to fibrosis [2].

Anti-fibrosis therapies target different stages of fibrotic progression, and the critical stage of hepatic fibrotic progression is sustained activation of HSCs caused by variant cytokines or signaling proteins [3-6]. As such, modulating the expression of cytokines and signaling proteins is essential for fibrotic blockade. Such treatment has gradually dominated anti-fibrotic therapies and attracted much attention in recent years [6-9].

Masson pine pollen is the male gametophyte of *Pinus massoniana lamb*, a Chinese endemic species. Masson pine pollen is a traditional

food that is often used in traditional medicine. It contains various proteins, multiple amino acids, 15 types of vitamins, more than 30 kinds of mineral elements, nearly 100 kinds of enzymes and coenzymes, >200 kinds of nucleic acids, unsaturated fatty acids, lecithin, flavonoids, choline, and so on [10, 11]. As such, Masson pine pollen has multiple benefits such as immunity enhancement, anti-aging, anti-fatigue, metabolism modulation, increasing hypolipidemic capacity, liver protection, blood glucose reduction, and skin protection.

Several reports recently demonstrated the liver protective effect of Masson pine pollen [12-14], and such an effect was associated with its antioxidant role [13]. Masson pine pollen protected against acute liver injury, and such protection may be derived from the alleviation of lipid peroxidation injury caused by alcohol, enhancement of fatty acid metabolism, and reduction of fat deposition in liver cells. Masson pine pollen could also promote liver function restoration and ascites absorption to benefit the treatment of liver diseases, especially chronic persistent hepatitis [12, 14].

We previously investigated the antioxidant function of Masson pine pollen *in vitro* [15, 16] and found that its extract could significantly delay the low-density lipoprotein oxidation induced by cupric ions. This may due to its chelation effect, which inhibited cupric ion-mediated induction, and its clearance effect of ROS, which blocked the fatty acid reactions to inhibit the lipid peroxidation process [8]. We also found that Masson pine pollen had the ability to scavenge various ROS [16].

Component analysis of Masson pine pollen revealed that crude fiber content is as high as 28.8%. As crude fiber is poorly soluble and forms a suspension in water, which hindered further clinical applications, extraction and enrichment of effective components could improve the effect of Masson pine pollen and promote its further uses. Higher total phenolic content is generally associated with higher antioxidant activity and might be the mechanism of its protective effects in the liver. Therefore, the total phenol content was measured using high-performance liquid chromatography and the result of the aqueous extract of pollen (19.81 mg/g) was much higher than that of the pollen original powder (0.38 mg/g) and ethanol extract (0.05 mg/g). However, Cheng et al [17] found that while ethanol extract had higher total phenolic content compared with water extract, its antioxidant activity was significantly lower than that of water extract. The difference in solvent polarity between ethanol and water may account for this since polysaccharides and low-molecular-mass proteins with antioxidant activities may exist in water extract [17, 18]. This study mainly focused on the effects and underlying pathways of Masson pine pollen aqueous extract (MPPAE) compared with Masson pine pollen original powder (MPPOP) in a hepatic fibrosis model and provided reliable experimental evidence for the preventive treatment of hepatic fibrosis and clinical applications of MPPAE.

Materials and methods

Extractions of Masson pine pollen extract powder: Fresh broken Masson pine pollen (purchased from New Era Health Industry (Group) Co. Ltd, Beijing, China.) was marinated in water for 30 min and extracted with ultrasonic waves for 30 min at normal temperature and pressure. The impurities were removed through centrifugation at 10,000 rpm/min for 15 min. The liquid supernatant was separated through ultrafiltration with molecular sieve at 1-5°C to obtain the aqueous extract with molecular weights < 3,000. Then it was freeze-dried to obtain the extract powder with a yield of approximately 15%.

Animal grouping and experimental design: This animal experiment was approved by the Experimental Animal Care and Use Committee of Academy of Military Medical Science. Sixty-one adult male Sprague-Dawley rats weighing 160-180 g each were randomly divided into five groups: normal control (CG), hepatic fibrosis (MG), MPPAE low dose (LG), MPPAE high dose (HG), and MPPOP (OP) groups. All of the rats were raised under environmentally controlled conditions at 23±1°C with 45±5% relative humidity under a 12-h light/dark cycle. The study groups and treatments are described in **Table 1**.

All rats were raised for 8 weeks. After a 12-h fast, the rats were anesthetized and exsangui-

Table 1. Study groups and treatments

Grouping	Number	Abdominal injection (0.3 mL/100 g once every 3 days)	Intragastric administration (1 mL/100 g once daily)
Normal control group (CG group)	10	saline solution	double distilled water
Hepatic fibrosis model group (MG group)	15	40% CCl_4	double-distilled water
MPPAE low dose group (LG group)	12	40% CCl_4	MPPAE 20 mg/mL (0.2 mg/g)
MPPAE high dose group (HG group)	12	40% CCl_4	MPPAE 100 mg/mL (1.0 mg/g)
MPPOP group (OG group)	12	40% CCl_4	MPPOP in double-distilled water 100 mg/mL (1.0 mg/g)

Table 2. Primer sequences of the four genes selected for real-time reverse transcription polymerase chain reaction using rat-act β as an internal control

Gene name	Primers (5'-3')
Rat-act b (bp711C)	*F: CTCATGCCATCCTGCGTCT*
Rat-act b (bp596)	*R: ACGCACGATTTCCCTCTCA*
TGF-β_1 (bp636)	*F: TGGAGCAACACGTAGAACTCTACC*
TGF-β_1 (bp764C)	*R: ACTGCCGGACAACTCCAGTG*
PDGF (bp992)	*F: TCGAGCCAAGACACCTCAA*
PDGF (bp1117C)	*R: GCTCCAAGGATCTCCTTCAGT*
α-SMA (bp275)	*F: TAGAACACGGCATCATCACC*
α-SMA (bp374C)	*R: AAGGTCGGATGCTCCTCTG*
NF-κB p65 (bp802)	*F: ACACTGGAAGCACGGATGAC*
NF-κB p65 (bp919C)	*R: TGTCTGTGAGTTGCCGGTCT*

F, forward primer; R, reverse primer; TGF-β_1, transforming growth factor-β_1; PDGF, platelet-derived growth factor; α-SMA, α-smooth muscle actin; NF-κB, nuclear factor-κB. The final results are expressed as normalized fold values relative to the CG.

nated. Blood were collected from the femoral aorta. Intact livers were removed, weighed immediately, and stored in liquid nitrogen for future experiments. In each group, three rats were killed and the livers were fixed in formaldehyde solution and embedded in paraffin for histopathological examination.

Measurement of liver index and biochemical assay

The liver index was calculated as liver weight divided by body weight. Blood was collected and centrifuged at 3,000× *g* for 10 min, and the serum was separated and stored at -70°C. The serum levels of aspartate transaminase (AST), alanine transaminase (ALT), and alkaline phosphatase (ALP) were determined using a Chemistry Analyzer (7600; Hitachi, Tokyo, Japan). Serum levels of hyaluronic acid (HA), laminin (LN), procollagen-III-peptide (PIIIP), and type IV collagen (IV-C) were detected using commercial radioimmunoassay kits (Beijing North Institute of Biological Technology, Beijing, China).

Histopathological examination and immunohistochemical staining

Liver tissues fixed in 10% neutral formalin solution for > 24 h were embedded in paraffin and cut into 4-μm-thick sections for histomorphological examination. After drying, liver tissue section slides were stained with hematoxylin and eosin (HE) and Masson's trichrome according to standard procedures for evaluating the degree of liver fibrosis.

Depending on the purpose of the experiment, following primary antibodies were used to label the tissue slices: anti α-SMA antibody (Abcam, Cambridge, UK), rabbit polyclonal anti-TGF-β_1 antibody(Abcam), and rabbit polyclonal anti-NF-κB p65 antibody (Abcam), After being washed three times with phosphate-buffered saline, the samples were incubated with goat anti-rabbit secondary monoclonal antibody (Sungene Biotech Co., Ltd., Tianjin, China) for 2 hours (at room temperature) to visualize immunolabeling results (streptavidin-peroxidase method).

Determination of hydroxyproline (Hyp) in liver tissues

Hyp determination was conducted using the alkali hydrolysis method [19]. Collagen level was calculated using the Hyp concentration as follows:

Collagen (μg/mg) = Hyp (μg/mg)/13.4%

Examination of oxidative stress

Lipid peroxidation in the liver was evaluated by measuring the formation of malondialdehyde (MDA) using the thiobarbituric acid reactive substances method. Activities of glutathione peroxidase (GSH-Px) and superoxide dismutase (SOD) in the liver were assayed using a com-

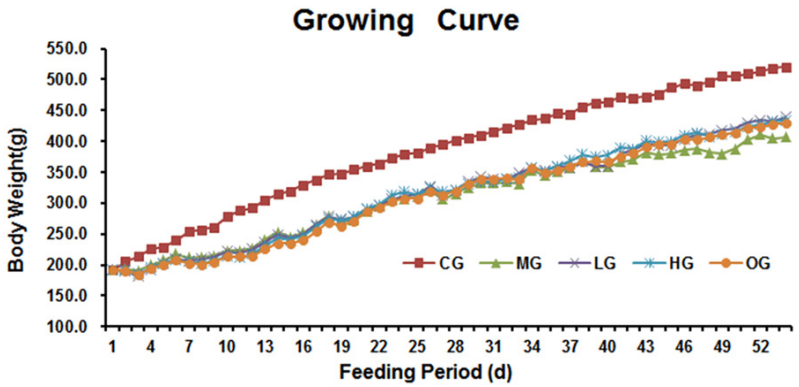

Figure 1. Rat growth curve. Growth curve showing that control group (CG) rats had the fastest growth rate (almost linear). Rats in the other groups grew tardy after CCl_4 treatment. The hepatic fibrosis model group (MG) rats grew the slowest from the middle to latter period.

Table 3. Body weights, liver weights, and liver indices by group

Group	n	Initial body weight (g)	Final body weight (g)	Liver weight (g)	Liver index (%)
CG	9	191.2±7.7	500.1±31.2^{c}	13.81±1.83	2.76±0.26^{a}
MG	10	191.7±8.3	380.0±51.1^{a}	15.83±2.93	4.15±0.39^{c}
LG	10	191.5±6.7	412.9±24.5^{a,b}	15.71±2.00	3.80±0.26^{b,c}
HG	10	191.4±8.7	414.6±19.1^{b}	14.97±1.19	3.61±0.39^{b}
OG	10	191.5±7.1	405.3±32.9^{a,b}	16.18±2.46	3.98±0.44^{b,c}

Values were showed as means ± SD (n was rat number). The different letters (a, b, c) corner marker between groups represents the statistic difference ($P < 0.05$). Same letter of corner marker showed no significant difference ($P > 0.05$) between groups. Data without corner letter were without statistic difference among groups.

mercial kit (Nanjing Jiancheng Bioengineering Institute, Nanjing, China). The 8-hydroxy-2'-deoxyguanosine (8-OH-dG) level in the liver was detected using a commercial enzyme-linked immunosorbent assay (ELISA) kit (Beijing North Institute of Biological Technology).

Measurement of MMP and TIMP expression

MMP-2, MMP-13, and TIMP-1 were analyzed using commercial ELISA kits (Abcam) according to the manufacturer's protocol.

Real-time polymerase chain reaction (PCR) for analyzing gene expression in liver tissues

Total RNA was isolated from RNA later-treated liver tissues using an RNeasy Mini Kit (Invitrogen, Carlsbad, CA, USA). Real-time PCR was performed using 7500 Fast (Life Technologies Corporation, Carlsbad, CA, USA) after cDNA synthesis. The primer sequences used were as follows (forward and reverse, respectively) in **Table 2**.

Statistical analysis

Quantitative data are expressed as mean ± standard deviation (n = 8-10). Differences between groups were analyzed using variance analysis of SPSS software (IBM Corporation, Armonk, NY, USA). In all analyses, values of $P < 0.05$ were considered statistically significant.

Results

Rat growth and liver index

The CG group rats grew well, while the rats in the other four groups showed obvious growth retardation (**Figure 1**). During the later period, ascites developed and deaths occurred in all of the model groups. In the MG group, the mortality rate and incidence of ascites were 33.3% and 50%, respectively, the highest of all four model groups, while the incidence of ascites was 16.7% in the LG group, 8.3% in the HG group and 16.7% in the OG group.

The rat weights were initially similar and no significant differences were observed among groups ($P>0.05$). When all experiments were completed, rat weight in the modeling groups was significantly lower than that in the CG group ($P < 0.01$), and compared with the CG group, the average rat weight in the MG group decreased by 24% (**Table 3**).

Histopathological examination of liver tissues

Histopathological section staining showed that in CG group rats, the structure of the hepatic lobules was normal, hepatic cells were orderly arranged, cytoplasmic staining was red and no vacuoles, hepatic turbidity, or fatty degeneration was seen in the cytoplasm. Masson's trichrome staining revealed low-density blue staining around the blood vessels. In the MG group rats, hepatic lobules could be observed but hepatic cords were irregular, ballooning

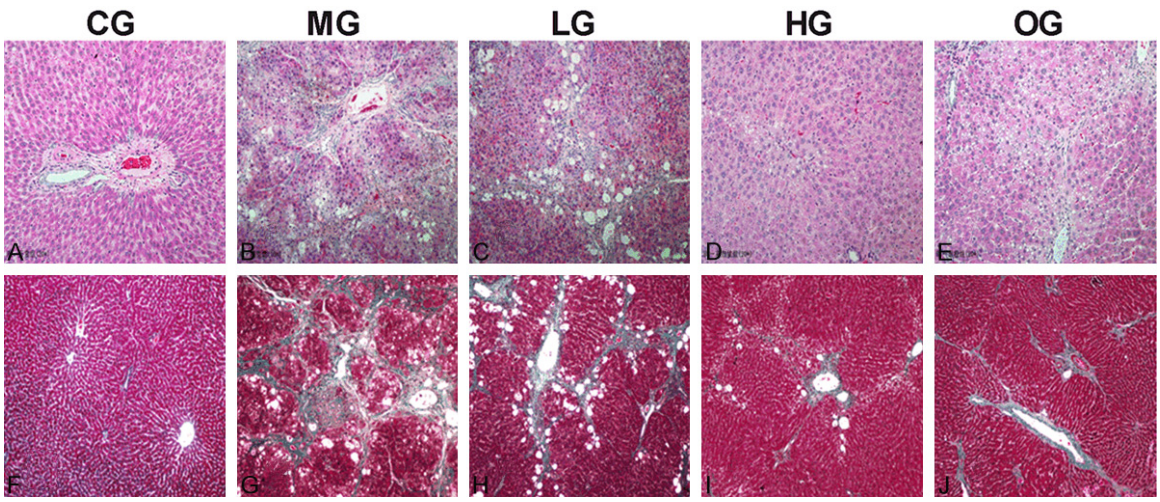

Figure 2. Hematoxylin and eosin (HE) and Masson staining of the liver slices. HE staining (A-E) of the liver tissues (100×); Control group (A): Hepatic lobule structure was normal, cells were orderly arranged, cytoplasmic staining was red, and no vacuoles or turbidity were seen. Model group (B): Hepatic lobules were visible, hepatic cords were irregular, and ballooning fatty degeneration was obvious in the hepatic cytoplasm. Masson pine pollen aqueous (MPPAE) low dose (LG), MPPAE high dose (HG), and Masson pine pollen original powder (MPPOP) groups (C-E): Conditions were significantly ameliorated according to MPPAE dose. Masson's trichrome stain (F-J): Red stain is cytoplasm, dark blue stain is nucleus, and cyan stain is collagen fibers. Control group (F): Only low-density cyan staining around the blood vessels. Model group (G): Collagen fiber hyperplasia intersected at multiple portal areas, collagen fiber bridging connected portal areas with central veins, leading to pseudolobuli formation. Cyan signals in the thick funicular fibers formed pseudolobuli within the parenchymal hepatic cells, indicating the successful establishment of the experimental hepatic fibrosis model. MPPAE low dose (LG), high dose (HG), and MPPOP (OG) groups (H-J): The cyan signals in the thick fibers were significantly weaker than those in the MG group.

Table 4. Alterations in serum biochemical parameters

Group	n	ALT (U/L)	AST (U/L)	ALP (U/L)
CG	9	28.2±7.2[a]	103.7±30.7[a]	138.2±29.4
MG	10	193.5±124.3[c]	458.6±226.9[b]	211.7±108.0
LG	10	85.3±46.4[b]	209.1±63.2[a]	149.9±52.9
HG	10	69.1±23.3[b]	192.4±78.4[a]	141.6±27.6
OG	10	99.9±53.8[b]	251.9±109.4[a]	194.3±65.0

Values were showed as means ± SD (n was rat number). The different letters (a, b, c) of corner marker between groups represent the statistic difference ($P < 0.05$). Same letter of corner marker showed no significant difference ($P > 0.05$) between groups. Data without corner letter was no statistic difference among all groups.

fatty degeneration was obvious in hepatic cytoplasm, inflammation appeared in portal areas with proliferation of small bile ducts, collagen fiber hyperplasia appeared and intersected at multiple portal areas, collagen fiber bridging connected portal areas with central veins, leading to pseudolobuli formation. In addition to positive signals around blood vessels, Masson's trichrome staining revealed blue signals in the thick funicular fibers out of the portal areas that formed pseudolobuli in parenchymal hepatic cells, indicating the successful establishment of this hepatic fibrosis rat model (**Figure 2**).

Ballooning degeneration was also observed in liver tissues of the LG, HG, and OG group rats, proliferation of fibrous connective tissue was apparent in the portal area, collagen fibers split hepatic lobules, bridging appeared but dramatic diffuse reduction was observed, pseudolobuli formation was not obvious, and the hepatic cords were nearly normal. Conditions in the HG group were better than those in the LG and OG groups; while Masson's trichrome staining revealed that blue signals in thick fibers were significantly weaker than those in the MG group.

Measurement of serum biochemical parameters associated with liver function

Significant upregulation of ALT and AST expressions were noted in the four modeling groups in compared with those in the CG group. ALT and AST levels increased 6.8-fold and 4.4-fold in the MG group compared to the CG group ($P < 0.01$), while MPPAE or MPPOP treatment

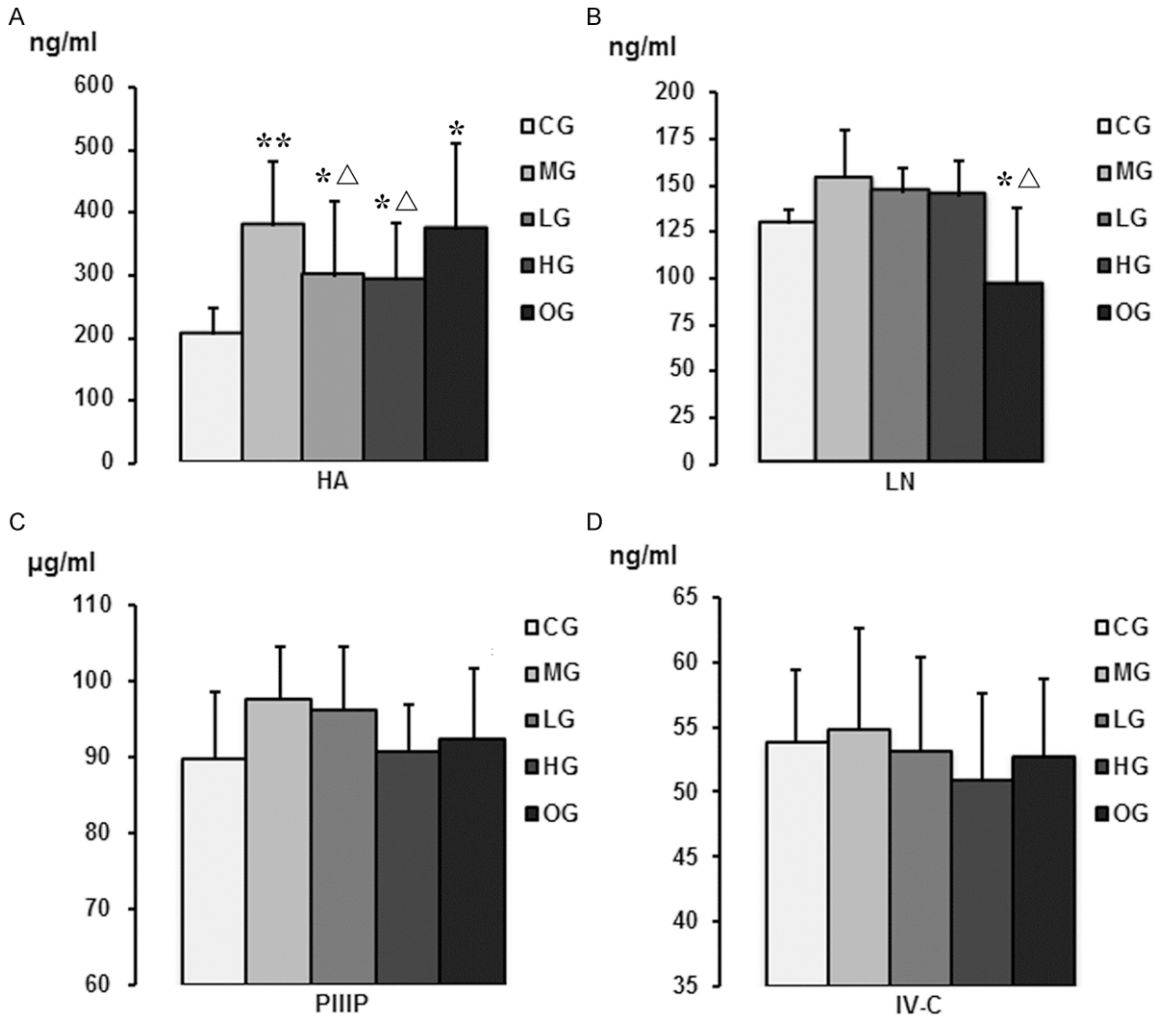

Figure 3. Four diagnostic indexes values of hyaluronic acid (HA) (A), laminin (LN) (B), procollagen-III-peptide (PIIIP) (C), and type IV collagen (IV-C) (D) of serumZ $*P < 0.05$ and $**P < 0.01$ vs. the normal group, $\Delta P < 0.05$ vs. the CCl_4 model group. The lack of a marker on the data bar indicates that the difference was not statistically significant ($P > 0.05$).

Table 5. Hyp and collagen content of the liver tissues

Group	n	Hyp (μg/mg)	Col (μg/mg)
CG	8	0.42±0.08[a]	3.10±0.61[a]
MG	8	0.76±0.18[c]	5.64±1.33[c]
LG	8	0.59±0.06[b,c]	4.42±0.43[b]
HG	8	0.58±0.29[b]	4.33±2.16[b]
OG	8	0.68±0.27[b,c]	5.05±2.04[b,c]

Values were showed as means ± SD (n was rat number). The different letters (a, b, c) of corner marker between groups represent the statistic difference ($P < 0.05$). Same letter of corner marker showed no significant difference ($P > 0.05$) between groups.

reduced the ALT and AST expressions by 55.9-64.3% and 54.4-58.0%, respectively, compared to the MG group ($P < 0.05$). ALP changed in similar ways, but the difference was not significant ($P > 0.05$) because of large individual differences (**Table 4**).

Measurement of four diagnostic serum indices for liver fibrosis

Compared with the CG group, the HA levels in other four model groups increased dramatically ($P < 0.05$). The MG group rats had a 1.85-fold increased HA expression and 8.54% PIIIP upregulation compared with the CG group. Compared with the MG group, HA expression was downregulated by 20.8% and 22.9% in the LG and HG groups, respectively, while PIIIP was downregulated by 7.1% in the HG group and

Table 6. Activity of antioxidant enzymes and peroxide products in the liver

Group	n	SOD (U/mg Prot)	MDA (nmol/mg Prot)	GSH-Px (U/mg Prot)	8-OH-dG (ng/mg Prot)
CG	8	29.71±3.77^{a,b}	0.75±0.12^{a,b}	293.52±33.11^{c}	2.16±0.43^{a}
MG	8	27.28±4.57^{a}	0.96±0.38^{b}	187.79±41.82^{a}	2.87±0.43^{b}
LG	8	29.99±5.24^{a,b}	0.72±0.12^{a,b}	204.78±27.75^{a,b}	2.58±0.44^{a,b}
HG	8	33.60±7.64^{b}	0.70±0.08^{a}	231.48±58.72^{b}	2.28±0.26^{a}
OG	8	31.33±6.50^{a,b}	0.77±0.14^{a,b}	194.09±32.82^{a}	2.57±0.30^{a,b}

Values were means ± SD (n was rat number). The different letters (a, b, c) of corner marker between groups represent the statistic difference ($P < 0.05$). Same letter of corner marker showed no significant difference ($P > 0.05$) between groups.

Table 7. MMP and TIMP expression in liver tissues

Group	n	MMP-2 (ng/mg)	MMP-13 (ng/mg)	TIMP-1 (ng/mg)
CG	8	1.90±0.24^{c}	3.88±0.76^{b,c}	1.46±0.28
MG	8	1.30±0.52^{a}	3.35±0.64^{a,b}	1.48±0.22
LG	8	1.61±0.25^{a,b}	3.50±0.90^{a,b}	1.43±0.48
HG	8	1.89±0.31^{c}	4.12±0.92^{c}	1.31±0.39
OG	8	1.71±0.26^{b,c}	4.17±0.67^{c}	1.00±0.49

Values were means ± SD (n was rat number). The different letters (a, b, c) of corner marker between groups represent the statistic difference ($P < 0.05$). Same letter of corner marker showed no significant difference ($P > 0.05$) between groups. Data without corner letter was no statistic different among all groups.

changed little in the LG and OG group ($P > 0.05$). LN and IV-C expression showed similar trends, but statistical analysis revealed no significant differences ($P > 0.05$) (**Figure 3**).

Collagen protein content in liver tissues

Compared with the CG group, collagen protein level increased 1.82-fold in the liver tissues in the MG group ($P < 0.01$). In the LG and HG groups, MPPAE treatment reduced collagen protein content significantly ($P < 0.05$). MPPOP treatment also improved collagen protein expression, but the difference was not statistically significant between the OG and MG groups ($P > 0.05$) (**Table 5**).

Assessment of antioxidant enzymes and peroxide products in the liver

In the liver tissues, SOD enzyme activity was lower in the MG group than in the CG group, while MPPAE or MPPOP treatment caused statistically significant increases in SOD activity in the HG and MG groups ($P < 0.05$). MDA and 8-OH-dG contents in liver tissues were higher in the MG group than in the CG group, whereas MPPAE treatment significantly reduced MDA and 8-OH-dG contents in the HG and MG groups ($P < 0.05$). Compared with CG group, GSH-Px activity was reduced by 36.0% in the MG group ($P < 0.01$), while MPPAE treatment significantly upregulated its activity in the HG and MG groups ($P < 0.05$) (**Table 6**).

MMP and TIMP expressions in liver tissues

Compared with the CG group, MMP-2 and MMP-13 expressions in the liver tissues were decreased by 31.6% and 13.6%, respectively, in the MG group ($P < 0.05$). MPPAE treatment significantly increased the expressions of MMP-2 and MMP-13 in a dose-dependent manner. However, MPPAE treatment decreased TIMP-1 expression, but no statistically significant difference was detected ($P > 0.05$) (**Table 7**).

Expression of α-SMA, NF-κB P65, and TGF-β_1 in liver tissues

Immunohistochemical experiments showed that α-SMA was barely detected in rat livers of the CG group, while weakly positive signals of NF-κB P65 and TGF-β_1 could be detected around blood vessels and appeared in a minority of hepatocytes, showing lower staining density. In the MG group rat liver tissues, all three cytokines were highly expressed and distributed mainly throughout the portal areas, fiber intervals, and hepatocytes. Pseudolobuli formed by fiber bridging was apparent due to the intensive staining density of these cytokines. MPPAE treatment significantly decreased the expression of these three cytokines in a dose-dependent manner. Expression reduction was also observed in the OG group but in a less obvious manner compared to that in the LG or HG groups (**Figure 4**).

mRNA expression of cytokine and signaling protein

Fluorescent qPCR experiments showed that the mRNA expression of TGF-β_1, NF-κB p65,

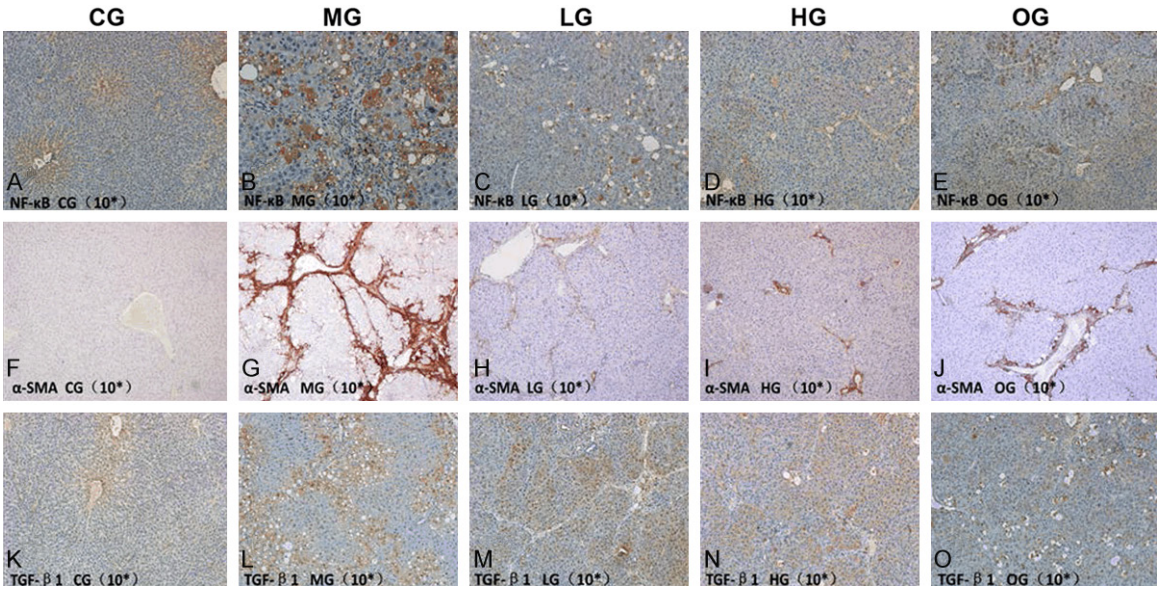

Figure 4. Immunohistochemical stain of nuclear factor-κB p65 (A-E), α-smooth muscle actin (F-J), and transforming growth factor-β_1 (K-O) in rat liver tissue (100×). Brown indicates specific Ab reactivity. In the CCl_4 treatment group (MG), NF-κB, α-SMA, and TGF-β_1 were remarkably upregulated, showing positive staining at the fibrotic septa, but downregulated in the experiment groups treated with pollen and its extract (low dose [0.2 mg/g, LG], high dose (1.0 mg/g [HG]) and original powder group (1.0 mg/g [OG]).

α-SMA, and platelet-derived growth factor (PDGF) were upregulated in the MG group compared with those in the CG group, and statistical significance was observed in α-SMA expression ($P < 0.05$). MPPAE or MPPOP treatment downregulated the mRNA expression of these four cytokines or signaling proteins in a dose-dependent manner. In fact, significant differences had been observed between the HG and MG groups ($P < 0.05$) (**Figure 5**).

Discussion

The liver, the body's largest substantial organ, is involved in multiple complicated physiological functions such as biogenesis, metabolism, transport, and excretion. Hepatic injury would lead to massive metabolic disturbances of proteins, lipids and saccharides. In the clinical setting, serum transaminase and liver fibrosis index are the most useful indicators of liver function and fibrosis, and the severity of hepatic fibrosis is directly related with collagen levels, which is often considered the endpoint of fibrosis analysis [20].

This study revealed the following: growth retardation is apparent in MG group rats, in which the liver index increased significantly; hyperplasia of fibrous connective tissues, hepatocyte ballooning, and steatosis were severe; the level of transaminases AST and ALT were obviously elevated in the serum; and collagen protein level increased abnormally. These results indicated that the CCl_4-induced hepatic fibrosis rat model was successfully established. We showed that MPPAE or MPPGP treatment alleviated CCl_4-induced hepatocyte toxicity, protected the liver histology and hepatocyte morphology, and functioned in a concentration-dependent manner. The MPPAE effect was superior to that of MPPOP, indicating that the active ingredients of Masson pine pollen are water soluble, and its effect was enhanced after purification, which increased the concentrations of the active ingredients.

Anti-fibrotic therapies currently focus on several aspects: inhibiting inflammation to reduce hepatocyte damage, blocking HSC activation by targeting cytokines such as TGF, PDGF, and mitogens to reduce ECM production and promote ECM degradation by targeting MMPs and TIMPs [21]. This study showed that Masson pine pollen extract arrested the progression of hepatic fibrosis through all three mechanisms mentioned above.

First of all, Masson pine pollen extract protected liver cells against oxidative damage by an

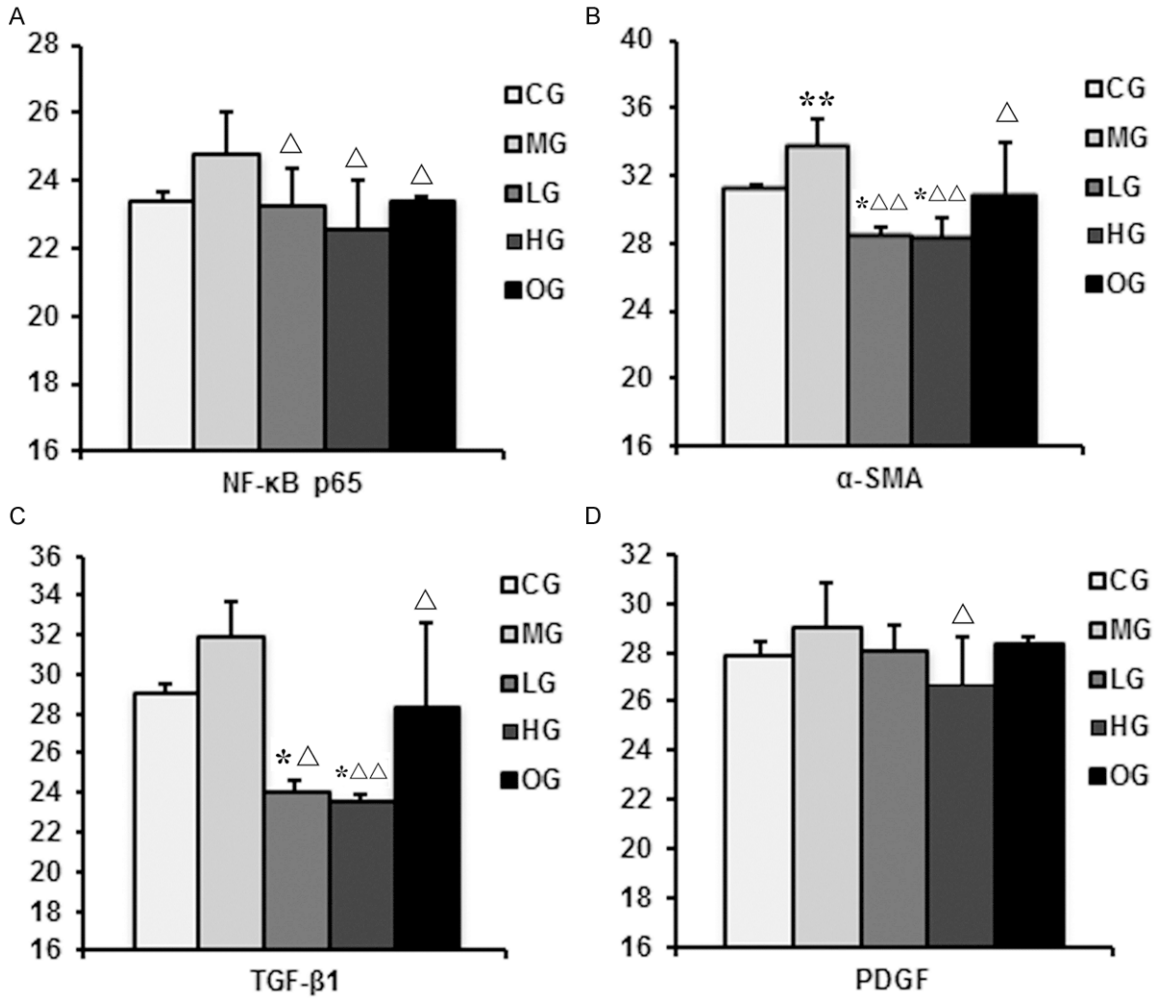

Figure 5. Expression levels of major liver fibrosis-associated genes. Y-axis value represents Ct of expression level of nuclear factor-κB p65 (A), α-smooth muscle actin (B), transforming growth factor-β1 (C), and platelet-derived growth factor (D) of quantitative polymerase chain reaction. *P < 0.05 and **P < 0.01 vs. the normal group, ΔP < 0.05 and ΔΔP < 0.01 vs. MG.

antioxidative pathway. CCl_4-induced hepatic injury is mainly associated with lipid peroxidation and an imbalance of intracellular calcium homeostasis, which produces oxygen free radicals through liver metabolism and initiates a secondary reaction that damages hepatocytes and leads to fatty degeneration and necrosis in liver cells [22]. MPPAE could not only increased GSH-Px activity but also efficiently cleared lipid peroxide MDA in the livers, protecting hepatocytes against oxygen free radicals and peroxides [13, 17].

ROS modification of DNA bases leads to DNA oxidative damage and is the critical factor of tumor development. We found that the level of 8-OH-dG, the characteristic product of DNA oxidative damage, was elevated dramatically in rat livers, indicating severe DNA oxidative damage in hepatocytes. MPPAE treatment significantly reduced the 8-OH-dG level, showing a protective effect against DNA damage [23].

Second, MPPAE promoted ECM degradation by regulating MMP expression. ECM is essential for liver fibrosis formation and MMPs are its major degrading enzymes, which accelerated ECM degradation to reverse the liver fibrosis. Human MMP-1 and rat MMP-13 are known as type I and III interstitial collagenase, while MMP-2 substrates include type IV collagen as well as other ECM components [21, 24]. MMPs expression could be modulated by TIMPs, and TIMP-1 is the inhibitor of MMP-1 and MMP-13. As such, TIMP-1 inhibition could promote the degradation of type I and III collagens. MPPAE

could effectively increase MMP-2 and MMP-13 expressions in liver tissues to promote ECM degradation and improve liver morphology; however, it has little impact on TIMP-1, indicating that it directly inhibits MMPs expression.

Finally, we found that MPPAE could regulate the expression of fibrosis-relevant cytokines to inhibit HSC activation and reduce ECM production. TGF-β_1, one of the most potent fibrosis-promoting factors and HSC agonists, promote the expression of ECM components while inhibiting ECM degradation and block MMPs production to reduce ECM degradation [25-28]. PDGF is the strongest mitogenic growth factor [29], and large amounts of PDGF stimulated the ERK1/2 and PAK-PI3K-Akt pathways and promoted HSC proliferation, leading to the transformation of HSCs to MFBs. As the specific biomarker of MFB, α-SMA expression increased with the progression of fibrosis and was closely associated with prognosis [29, 30]. NF-κB, a transcriptional activator, is closely related to inflammation and tissue fibrosis. Studies have indicated that elevated NF-κB expression activated numerous target genes, leading to HSC activation and fibrosis progression [31]. Immunohistochemical experiments clearly showed that MPPAE treatment inhibited the abnormal expression of related cytokines. Finally, the qPCR results provided further evidence that MPPAE may arrest fibrosis progression by modulating cytokine and nuclear factor-κB expression to inhibit HSC activation and ECM production.

All results suggest that Masson pine pollen aqueous extract has anti-fibrosis effect on experimental liver fibrosis induced by CCl_4. The effective way include antioxidative protection , inhibitory activity on HSC proliferation and collagen synthesis, down regulation of relevant cytokines and nuclear factor such as TGF-β_1, PDGF, NF-κB p65, and signaling protein α-SMA up regulation of MMPs expression. However deeper studies need to be done to clarify more specific molecular mechanism.

Disclosure of conflict of interest

None.

Address correspondence to: Ping Zhao, International Center for Liver Disease Treatment, 302 Hospital of PLA, Beijing 100039, China. Tel: +86-1352196-8706; Fax: +86-21-64085875; E-mail: zhaop9262@sina.com; Chang-Jiang Guo, Department of Nutrition, Institute of Health and Environmental Medicine, Tianjin 300050, China. Tel: +86-13521968706; Fax: +86-21-64085875; E-mail: guocjtj@126.com

References

[1] Friedman SL. Molecular regulation of hepatic fibrosis, an integrated cellular response to tissue injury. J Biol Chem 2000; 275: 2247-50.

[2] Sato M, Suzuki S and Senoo H. Hepatic stellate cells: unique characteristics in cell biology and phenotype. Cell Struct Funct 2003; 28: 105-12.

[3] Biernacka A, Dobaczewski M and Frangogiannis NG. TGF-beta signaling in fibrosis. Growth Factors 2011; 29: 196-202.

[4] Kang KH, Qian ZJ, Ryu B, Karadeniz F, Kim D and Kim SK. Hepatic Fibrosis Inhibitory Effect of Peptides Isolated from Navicula incerta on TGF-beta1 Induced Activation of LX-2 Human Hepatic Stellate Cells. Prev Nutr Food Sci 2013; 18: 124-32.

[5] Liu T, Wang X, Karsdal MA, Leeming DJ and Genovese F. Molecular serum markers of liver fibrosis. Biomark Insights 2012; 7: 105-17.

[6] Wynn TA. Cellular and molecular mechanisms of fibrosis. J Pathol 2008; 214: 199-210.

[7] Bataller R and Brenner DA. Liver fibrosis. J Clin Invest 2005; 115: 209-18.

[8] Friedman SL. Hepatic stellate cells: protean, multifunctional, and enigmatic cells of the liver. Physiol Rev 2008; 88: 125-72.

[9] Le Bousse-Kerdiles MC, Martyre MC and Samson M. Cellular and molecular mechanisms underlying bone marrow and liver fibrosis: a review. Eur Cytokine Netw 2008; 19: 69-80.

[10] Chen W, Han XF, Lu JG, Liu WW, Tian YH and Wu XR. Determination of 16 elements in the different pine pollen by TXRF. Guang Pu Xue Yu Guang Pu Fen Xi 2012; 32: 2250-3.

[11] Wang YM, Wang HJ and Zhang ZY. Analysis of pine pollen by using FTIR, SEM and energy-dispersive X-ray analysis. Guang Pu Xue Yu Guang Pu Fen Xi 2005; 25: 1797-800.

[12] Cheng N, Ren N, Gao H, Lei X, Zheng J and Cao W. Antioxidant and hepatoprotective effects of Schisandra chinensis pollen extract on CCl_4-induced acute liver damage in mice. Food Chem Toxicol 2013; 55: 234-40.

[13] Lee KH, Kim AJ and Choi EM. Antioxidant and antiinflammatory activity of pine pollen extract in vitro. Phytother Res 2009; 23: 41-8.

[14] Saric A, Balog T, Sobocanec S, Kusic B, Sverko V, Rusak G, Likic S, Bubalo D, Pinto B, Reali D and Marotti T. Antioxidant effects of flavonoid from Croatian Cystus incanus L. rich bee pollen. Food Chem Toxicol 2009; 47: 547-54.

[15] Bao SF, Cong T, Illig J, Schempp H and Elstner EF. The experiment study in vitro on antioxidant properties of pinus masson pollen. Acta Nutrimenta Sinica 2005; 27: 487-90.
[16] Bao SF, Cong T, Illig J, Schempp H and Elstner EF. Study on the an tioxidant properties and mechanism of pollen and needle extracts from pinus massoniana in lipophilic model system. Academic Journal of PLA Postgraduate Medical School 2006; 27: 381-3.
[17] Cheng N, Gao H, Wang BN, Deng JJ, Liu YY and Cao W. Antioxidant Activities and Phenolic Compounds of the Pine Pollen Extracts. Food and Fermentation Industries 2007; 7: 401-8.
[18] Yang X, Guo D, Zhang J and Wu M. Characterization and anti-tumor activity of pollen polysaccharide. Int Immunopharmacol 2007; 7: 401-8.
[19] Reddy GK and Enwemeka CS. A simplified method for the analysis of hydroxyproline in biological tissues. Clin Biochem 1996; 29: 225-9.
[20] Liu CH. Detection evolve and estimation of collagen in liver. World Chinese Journal of Digestology 2003; 6: 1-4.
[21] Ahmad A and Ahmad R. Understanding the mechanism of hepatic fibrosis and potential therapeutic approaches. Saudi J Gastroenterol 2012; 18: 155-67.
[22] Helbock HJ, Beckman KB and Ames BN. 8-Hydroxydeoxyguanosine and 8-hydroxyguanine as biomarkers of oxidative DNA damage. Methods Enzymol 1999; 300: 156-66.
[23] Fujii T, Fuchs BC, Yamada S, Lauwers GY, Kulu Y, Goodwin JM, Lanuti M and Tanabe KK. Mouse model of carbon tetrachloride induced liver fibrosis: Histopathological changes and expression of CD133 and epidermal growth factor. BMC Gastroenterol 2010; 10: 79.
[24] Cheng K and Mahato RI. Gene modulation for treating liver fibrosis. Crit Rev Ther Drug Carrier Syst 2007; 24: 93-146.
[25] Borkham-Kamphorst E, van Roeyen CR, Ostendorf T, Floege J, Gressner AM and Weiskirchen R. Pro-fibrogenic potential of PDGF-D in liver fibrosis. J Hepatol 2007; 46: 1064-74.
[26] Cheng K, Yang N and Mahato RI. TGF-beta1 gene silencing for treating liver fibrosis. Mol Pharm 2009; 6: 772-9.
[27] Hellerbrand C, Stefanovic B, Giordano F, Burchardt ER and Brenner DA. The role of TGF beta1 in initiating hepatic stellate cell activation in vivo. J Hepatol 1999; 30: 77-87.
[28] Shek FW and Benyon RC. How can transforming growth factor beta be targeted usefully to combat liver fibrosis? Eur J Gastroenterol Hepatol 2004; 16: 123-6.
[29] Clouston AD, Jonsson JR, Purdie DM, Macdonald GA, Pandeya N, Shorthouse C and Powell EE. Steatosis and chronic hepatitis C: analysis of fibrosis and stellate cell activation. J Hepatol 2001; 34: 314-20.
[30] Khan MA, Poulos JE, Brunt EM, Li L, Solomon H, Britton RS, Bacon BR and Di Bisceglie AM. Hepatic alpha-smooth muscle actin expression in hepatitis C patients before and after interferon therapy. Hepatogastroenterology 2001; 48: 212-5.
[31] Baldwin AS Jr. The NF-kappa B and I kappa B proteins: new discoveries and insights. Annu Rev Immunol 1996; 14: 649-83.